Catalysis Today 148 (2009) 268–274

Contents lists available at ScienceDirect

Catalysis Today

journal homepage: www.elsevier.com/locate/cattod

Research on Ni/γ-Al_2O_3 catalyst for CO_2 reforming of CH_4 prepared by atmospheric pressure glow discharge plasma jet

Shuyong Shang [a,b], Gaihuan Liu [a,c], Xiaoyan Chai [a], Xumei Tao [a], Xiang Li [a,d], Meigui Bai [a], Wei Chu [a], Xiaoyan Dai [a], Yanxi Zhao [e], Yongxiang Yin [a,*]

[a] Center of Plasma Application, School of Chemical Engineering, Sichuan University, 24, South Section 1, Yihuan Road, Chengdu, Sichuan 610065, China
[b] Department of Chemical Engineering, Yibin University, Yibin, Sichuan 644007, China
[c] China Petroleum Engineering Co., Ltd Southwest Co., Chengdu, Sichuan 610017, China
[d] College of Science, Southwest University of Science and Technology, Mianyang, Sichuan 621010, China
[e] College of Chem. and Mater., South China University of Nationalities, Wuhan, Hubei 430074, China

ARTICLE INFO

Article history:
Available online 29 October 2009

Keywords:
Atmospheric pressure glow discharge plasma jet
Plasma-assisted
Ni/γ-Al_2O_3 catalyst
Methane
Carbon dioxide
Reforming

ABSTRACT

Ni/γ-Al_2O_3 catalyst had been prepared by atmospheric pressure glow discharge (APGD) plasma jet. Such plasma-prepared catalyst exhibited an improved low-temperature activity in CO_2 reforming of CH_4, compared to that of the catalyst prepared by conventional method. Characteristics of catalysts were analyzed by means of X-ray powder diffraction (XRD), temperature programmed desorption (TPD) experiment with H_2 or CO_2 probe, Brunauer–Emmett–Teller (BET) procedure, transmission electron microscopy (TEM) and thermogravimetric analysis (TGA). The XRD and TEM characterization showed that this novel plasma-assisted preparation induced Ni nano-particles as small as 5 nm. The results of XRD, H_2-TPD and TEM confirmed that, the nickel dispersion of the Ni/γ-Al_2O_3 catalyst by APGD was enhanced greatly. The improved anti-coke deposition performance was illustrated from the results of TGA, CO_2-TPD and the stability test experiments.

1. Introduction

The reaction of CO_2 reforming of CH_4 from two greenhouse gases to synthesis gas, a mixture of hydrogen and carbon monoxide, with its attracting industrial value and positive environment implication, had been of a great interest to the researchers. Intensive efforts had been devoted to investigate the more suitable catalyst for this reaction [1–12]. Nickel-based catalyst, among the investigated catalysts, was much promising for practical application because of its high activity and low cost. Therefore, a lot of works had been done to promote its low-temperature activity and coking-resistant ability. The effects of different promoters [1–5], supports [6–9] and preparing procedures [10–12] were investigated in order to improve its catalytic performance.

In recent years, the plasma technology had been employed to prepare new efficient catalyst because of its unique efficiency in the catalyst activation [10–33]. Vissokov et al. applied the electric arc plasma to the synthesis and regeneration of catalysts for natural gas reforming [13,14]. Phillips et al. studied generation of the supported Pd/C, Pd/Al_2O_3 catalysts by plasma torch [15,16]. Liu et al. investigated several plasma-assisted catalysts, e.g., Ni/Al_2O_3 [12,17,18], Ir/Al_2O_3 [19], Ni/SiO_2 [20], Pd/HZSM-5 [21], Pt/NaZSM [22] and Rh/Al_2O_3 [23], with a method that the catalyst was firstly treated by vacuum glow discharge and then thermally calcined, and made a conclusion of the remarkable enhancement in the dispersion and low-temperature activity of the catalysts [24]. Chu et al. explored several glow discharge plasma-assisted new catalysts [25–28], such as the plasma-enhanced Ni/γ-Al_2O_3 [25], Ni/α-Al_2O_3 [26], Fischer–Tropsch cobalt catalysts [27] and Pd/α-Al_2O_3 samples [28]. These catalysts were treated by a radio frequency plasma, and there were higher catalytic performances than those of the catalysts prepared by thermal treatment. The applications of other plasma techniques, e.g., dielectric-barrier discharge [29], microwave plasma [30], corona discharge [31], induction discharge [32] and plasma-spraying technology [33] were also reported in the catalyst preparation.

In our previous works, the performances of plasma-enhanced nickel-based catalysts were investigated [10,11], and the advantages of the novel APGD plasma jet were presented, especially the PC&R method [11]. As the SiO_2-supported nickel catalyst was easily deactivated in CO_2 reforming of CH_4 [4,34,35] and the γ-Al_2O_3 sample was a more promising support [6,8], the new PC&R method was introduced to prepare the more efficient Ni/γ-Al_2O_3 catalyst in our work. The steps of conventional calcination and thermal reduction were omitted during the preparation process,

* Corresponding author. Tel.: +86 13348865689.
E-mail addresses: hyyx0675@sina.com, ssyandmltcdj@163.com (Y. Yin).

0920-5861/$ – see front matter.
doi:10.1016/j.cattod.2009.09.011

and only APGD plasma jet was employed to decompose and reduce the catalyst precursor. Besides, the new samples prepared by this plasma technique were characterized and analyzed by XRD, H_2-TPD, CO_2-TPD, TEM, and TGA techniques. The catalytic performances in the reaction of CO_2 reforming of CH_4, as well as the coke formation during reaction and the primary stability of these samples were also investigated.

2. Experimental

2.1. Sample preparation

The 12%Ni/γ-Al_2O_3 catalysts were prepared by three methods, using conventional thermal method (C) for comparison, PR method and PC&R method.

The preparation procedures: the γ-Al_2O_3 support was first impregnated with an aqueous solution of $Ni(NO_3)_2$ and dried at 110 °C for 5 h. Then it was divided into three parts. The first part for C sample was calcined at 550 °C for 5 h, and the resulting material was reduced at 750 °C in pure hydrogen for 2 h; The second for PR sample was conventionally calcined at 550 °C for 5 h, then reduced by plasma jet for 10 min; The third for PC&R sample was directly decomposed and reduced by plasma jet for 10 min.

Fig. 1 presented APGD plasma jet for catalysts preparation. An inside copper stick was connected to the high voltage supply. The coaxial stainless steel crust served as the grounded electrode. 20%H_2/Ar with a flux of 1.5 m^3/h was applied as the plasma-forming gas. When 20 kHz AC voltage was utilized, the plasma gas was jetted into the catalyst bed. Under the discharging conditions, the temperature of the catalyst bed was 527 °C.

2.2. Catalyst evaluation and characterization

2.2.1. Catalyst evaluation

The catalytic evaluation was carried out in a fixed-bed reactor under 600–900 °C, a fixed CH_4/CO_2 molar ratio of 4/6, and GHSV of 30 L/(g h). The GC7900 gas chromatograph (Shanghai Techcomp Instrument Ltd., China; the chromatographic column was TDX-01) was used to analyze the products. The conversions of methane and carbon dioxide, the yields of hydrogen and CO were defined habitually.

2.2.2. XRD measurement

XRD patterns of samples were carried out in the DX-2500 (Dandong, China) diffractometer by using a Cu Kα radiation at 36 kV and 28 mA. The scan rate was 0.11°/10 s for 2θ ranging from 15° to 95°. The average nickel crystallite diameter was calculated by using Scherrer equation from all the Ni peaks.

$$d = \frac{0.89\lambda}{B\cos\theta} \times \frac{180^\circ}{\pi}$$

where d is the mean crystallite diameter, λ is the X-ray wavelength, and B is the full width half maximum (FWHM) of the Ni diffraction peak.

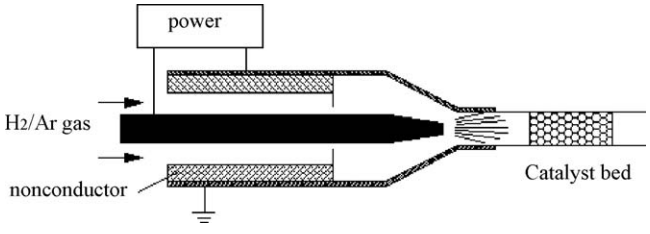

Fig. 1. Schematic of apparatus for APGD plasma jet.

2.2.3. H_2-TPD measurement

TPD experiment was carried out in a quartz tube. The sample (100 mg) was first held at 373 K for 1 h under flowing argon to remove physisorbed and/or weakly bound species. H_2 adsorption was occurring at 373 K by passing 10% (vol) H_2/Ar mixed gas with a flow rate of 30 ml/min into the adsorption instrument. The TPD signal was recorded with the temperature increasing at a rate of 10 °C/min to 800 °C.

Based on the assumption that the H:Ni stoichiometric ratio was 1:1, the Ni dispersion could be calculated according to the TPD spectra [36,37].

$$D\,(\%) = \frac{N_{\text{surface}}}{N_{\text{total}}} \times 100 = \frac{N_{H_2} \times 2}{N_{\text{total}}} \times 100$$

Here,

$$N_{H_2}\,(\text{mol}) = \frac{S_{\text{TPD}}(V_{\text{loop}}/S_{\text{pulse}})}{24.5 \times 10^3\ \text{ml/mol}}$$

where N_{surface} is the mole number of nickel on the surface of catalysts, mol; N_{total} is the total mole number of nickel in the sample, mol; D is the catalyst dispersion; N_{H_2} is the mole number of H_2 uptake, mol; 24.5 is the mole volume of gas at the room temperature of 25 °C; S_{TPD} is the analytical area from TPD; V_{loop} is the loop calibration volume, ml; and S_{pulse} is the mean area of hydrogen pulses.

2.2.4. CO_2-TPD measurement

The sample (100 mg) was firstly held at 573 K for 1 h under flowing argon to remove physisorbed and/or weakly bound species. CO_2 adsorption was occurring at room temperature by passing 10% (vol) CO_2/Ar mixed gas with a flow rate of 30 ml/min into the adsorption instrument. The TPD signal was recorded with the temperature increasing to 800 °C at a rate of 10 °C/min.

2.2.5. BET characterization

The specific surface area and pore size distribution of the catalysts were determined by nitrogen adsorption by using a NOVA 1000e apparatus (Quantachrome, USA) at 77.35 K. The specific surface area was calculated by using the BET method while the pore size distribution was obtained from the adsorption isotherm by method of Barrett, Joyner and Halenda (BJH).

2.2.6. TEM analysis

TEM analysis was performed on a TECNAI G^2 20 S-Twin (FEI, USA) TEM apparatus.

2.2.7. TGA characterization

TGA was performed in a TGA Q500 thermal analyzer. Air at flow rate of 50 ml/min was introduced into the instrument. Sample was loaded onto the thermo-balance and heated to 800 °C at a rate of 15 °C/min until a constant weight was obtained. The weight loss was recorded simultaneously.

3. Results and discussion

3.1. Catalytic performance

The catalytic activity of the Ni/γ-Al_2O_3 catalysts prepared by the three different methods was shown in Tables 1 and 2 with the reaction temperature varying from 650 °C to 850 °C. Though both of the conversions of CH_4, CO_2 and the yields of H_2, CO increased over the experimental temperature region for three kinds of catalysts, the plasma-assisted catalysts exhibited better catalytic performance, compared to the conventional catalyst. Especially the Ni/γ-Al_2O_3 catalyst by the PC&R method presented excellent low-temperature activity.

Table 1
CH_4 and CO_2 conversions over the different Ni/γ-Al_2O_3 catalysts.

Catalyst	Conversion (%)									
	650 °C		700 °C		750 °C		800 °C		850 °C	
	CH_4	CO_2	CH_4	CO_2	CH_4	CO_2	CH_4	CO_2	CH_4	CO_2
Ni/γ-Al_2O_3 (C)	36.4	35.0	48.5	42.8	62.9	52.4	80.3	64.4	91.6	69.7
Ni/γ-Al_2O_3 (PR)	39.2	37.2	51.7	46.0	67.2	57.8	85.4	69.1	95.8	75.7
Ni/γ-Al_2O_3 (PC&R)	43.7	36.9	60.9	50.0	79.7	61.6	94.2	73.8	98.4	80.6

Reactions conditions: catalyst 200 mg, Ni loading 12%, GHSV = 30 L/(g h) and CH_4/CO_2 molar ratio = 4/6.

Table 2
H_2 and CO yields (%) over the different catalysts.

Catalyst	Yield (%)									
	650 °C		700 °C		750 °C		800 °C		850 °C	
	H_2	CO	H_2	CO	H_2	CO	H_2	CO	H_2	CO
Ni/γ-Al_2O_3 (C)	34.7	33.5	47.0	40.9	62.0	51.8	79.1	62.9	90.1	67.7
Ni/γ-Al_2O_3 (PR)	37.5	35.9	50.3	44.5	66.2	56.7	84.0	68.1	94.3	74.1
Ni/γ-Al_2O_3 (PC&R)	42.9	36.0	59.8	49.1	79.1	61.3	93.7	72.7	97.9	79.5

Reactions conditions: catalyst 200 mg, Ni loading 12%, GHSV = 30 L/(g h) and CH_4/CO_2 molar ratio = 4/6.

3.2. XRD results

Fig. 2 presented the XRD patterns of the Ni/γ-Al_2O_3 (C), Ni/γ-Al_2O_3 (PR) and Ni/γ-Al_2O_3 (PC&R) samples. From Fig. 2A, the conventional Ni/γ-Al_2O_3 owned the peaks with d = 2.04, 1.76, 1.25, 1.06 which were assigned to metallic Ni phase, and the peaks with d = 4.60, 2.81, 2.41, 1.99, 1.52, 1.41, 1.15 which were assigned to alumina phase. For the plasma-activated Ni/γ-Al_2O_3 (PR) and Ni/γ-Al_2O_3 (PC&R) catalysts, the metallic Ni phase and the alumina phase also could be seen, as shown in Fig. 2B and C. But the nickel characteristic peaks of the plasma-assisted samples were much broader, compared to those of the Ni/γ-Al_2O_3 (C) catalyst. This indicated that the Ni particle size of Ni/γ-Al_2O_3 (PR) and Ni/γ-Al_2O_3 (PC&R) was smaller than that of Ni/γ-Al_2O_3 (C). The nickel particle size of the three samples was calculated by Scherrer formula. The Ni size was 17.8 nm for Ni/γ-Al_2O_3 (C), but it was only 5.4 nm for Ni/γ-Al_2O_3 (PR) and 5.0 nm for Ni/γ-Al_2O_3 (PC&R). The smaller nickel particle size inevitably brought about increasing in Ni dispersion and higher activity as well as better anti-carbon deposit performance of the catalyst, which was responded by following experiments.

3.3. H_2-TPD characterization

H_2-TPD curves for 12%Ni/γ-Al_2O_3 catalysts prepared by various methods were presented in Fig. 3. Peak A presented a very weak form of molecular adsorption below 200 °C. Peaks B and C were related to very strong bound chemisorption sites. From Fig. 3, the chemisorbed hydrogen amount increased in accordance with the order of Ni/γ-Al_2O_3 (C), Ni/γ-Al_2O_3 (PR) and Ni/γ-Al_2O_3 (PC&R), which showed that the Ni/γ-Al_2O_3 (PC&R) samples exhibited largest hydrogen adsorption capacity, and the conventional sample showed the least.

The Ni dispersion data calculated according to the TPD spectra were listed in Table 3. The conventional Ni/γ-Al_2O_3 (C) catalyst presented a Ni dispersion of 14.7%, while it was 22.1% and 30.6% for the plasma-activated Ni/γ-Al_2O_3 (PR) and Ni/γ-Al_2O_3 (PC&R) catalysts, respectively. The results showed that the application of the plasma jet greatly improved the hydrogen adsorption capacity of Ni/γ-Al_2O_3 catalyst, and more active sites existed over the surface of the catalysts, especially the Ni/γ-Al_2O_3 catalyst by the PC&R method, which was in good agreement with the results obtained from the XRD characterization.

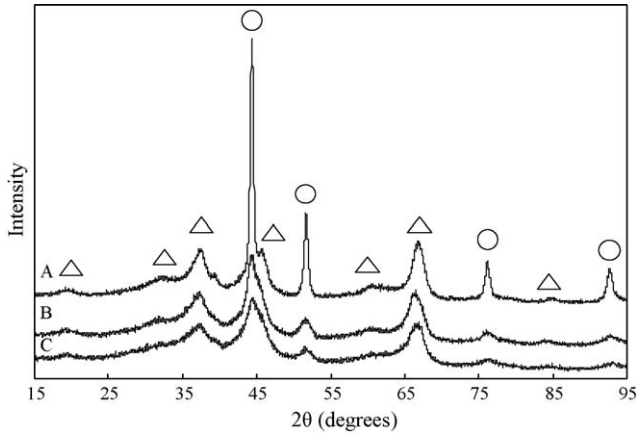

Fig. 2. XRD patterns of the 12%Ni/γ-Al_2O_3 catalysts. (A) C, (B) PR and (C) PC&R; (△) Al_2O_3 and (○) Ni.

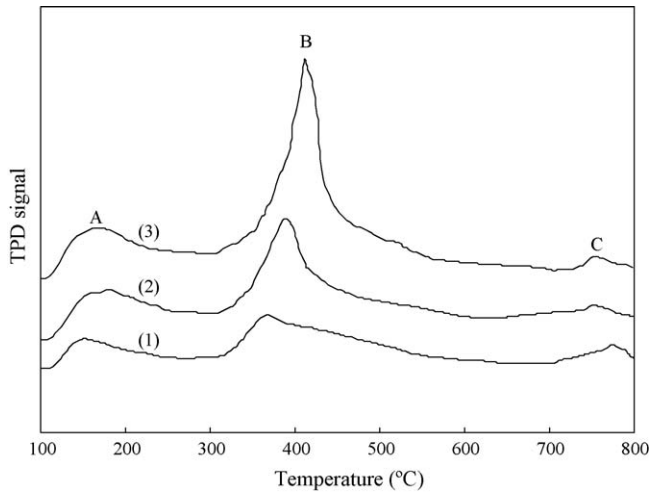

Fig. 3. H_2-TPD patterns of the Ni/γ-Al_2O_3 samples prepared by different methods. (1) C, (2) PR and (3) PC&R.

Table 3
H_2-TPD results of Ni/γ-Al_2O_3 samples prepared by different methods.

Samples	H_2 desorbed (μmol/g)	Dispersion (%)
Ni/γ-Al_2O_3 (C)	150.7	14.7
Ni/γ-Al_2O_3 (PR)	225.8	22.1
Ni/γ-Al_2O_3 (PC&R)	312.5	30.6

TPD results presented a nickel dispersion with the order of Ni/γ-Al_2O_3 (C) < Ni/γ-Al_2O_3 (PR) < Ni/γ-Al_2O_3 (PC&R), which could be attributed to the different treatment processes. For Ni/γ-Al_2O_3 (C) sample, the metallic nickels were easily sintered and conglomerated during the long-time, high-temperature process, such as calcination at 550 °C for 5 h and reduction at 750 °C for 2 h. For Ni/γ-Al_2O_3 (PC&R) sample, there were large amount of H atoms and other high-energy particles in the plasma jet, so it could decompose the precursor of $Ni(NO_3)_2$/γ-Al_2O_3 and reduce the NiO/γ-Al_2O_3 effectively in a kindly temperature environment and shorter process time, and avoid the conglomeration and sintering of the metallic nickel. At the meantime, the bombardment of the charged particles in the plasma jet on the surface of catalysts also benefited nickel dispersion. As a result, the Ni/γ-Al_2O_3 (PC&R) sample presented higher Ni dispersion with the average nickel diameter of only 5 nm.

3.4. CO_2-TPD characterization

CO_2-TPD curves for 12%Ni/γ-Al_2O_3 catalysts prepared by three methods were presented in Fig. 4. Peak A presented a weak Lewis alkaline site adsorbed at 100 °C. Peak B presented a strong Lewis alkaline site adsorbed at 400–500 °C.

The chromatographic areas of peaks A and B calculated according to the CO_2-TPD spectra of three samples were listed in Table 4. Obviously, the B-peak areas of Ni/γ-Al_2O_3(C) catalyst were smaller than those of Ni/γ-Al_2O_3 (PR and PC&R) catalysts. Compared to the conventional catalyst, the areas of A-peak and B-peak of PC&R catalysts were increased about 71.2% and 165.7%, respectively. Li et al. [38] reported CO_2 adsorption took place on the support surface but not on the Ni particle. Because CO_2 was acid gas, it could only be adsorbed on the alkaline site of support surface. The increase in peak areas of CO_2-TPD showed that the alkalescence of support surface treated by plasma was improved significantly. It benefited to the carbon deposition elimination and increased the coking-resistant ability of catalyst surface.

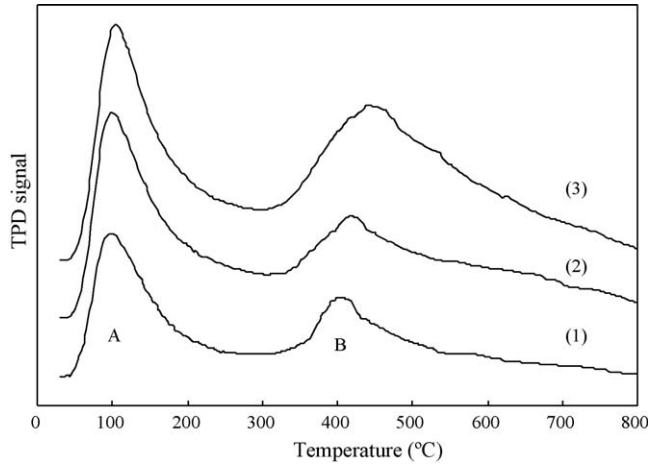

Fig. 4. CO_2-TPD patterns of the Ni/γ-Al_2O_3 catalysts. (1) C, (2) PR and (3) PC&R.

Table 4
CO_2 desorption peak area over different Ni/γ-Al_2O_3 samples.

Sample	CO_2 desorption peak area (a.u.)	
	Peak A	Peak B
12%Ni/γ-Al_2O_3 (C)	7.98	6.06
12%Ni/γ-Al_2O_3 (PR)	11.84	9.66
12%Ni/γ-Al_2O_3 (PC&R)	13.66	16.10

3.5. BET characterization

N_2 adsorption experimental results were shown in Fig. 5. The difference in the pore size of Ni/γ-Al_2O_3 (PC&R), Ni/γ-Al_2O_3 (PR) and Ni/γ-Al_2O_3 (C) was significant. It seemed strange that, from Table 5 and the pore size distribution curves, the average pore diameter of the three Ni/γ-Al_2O_3 catalysts had an increase compared to that of the γ-Al_2O_3 support, especially, the most obvious change in average pore diameter of Ni/γ-Al_2O_3 (C) was from 5.8 nm to 9.8 nm. It was probably due to the sintering of support and the diffusing of Ni particle into support pores with smaller size. Because the sintering of support produced larger pores, the diffusing of Ni particle into support plugged the smaller pores, both brought about the changes of pore size distribution of catalysts, as shown in Fig. 5, so the average pore diameter of the three Ni/γ-Al_2O_3 catalysts changed. However, Ni/γ-Al_2O_3 (PC&R) sample, due to shorter treatment time and omitting of long-time,

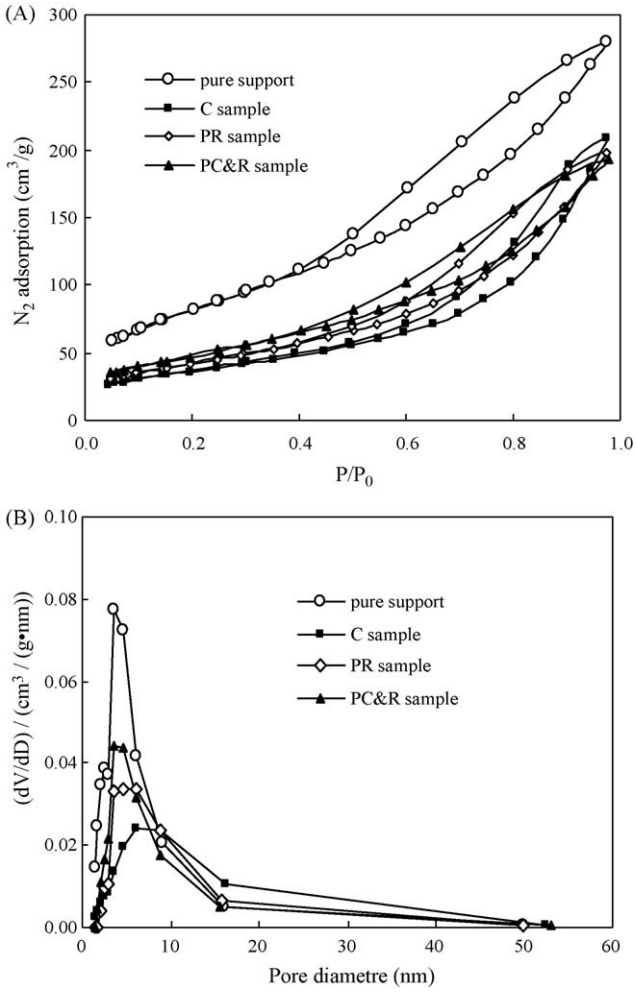

Fig. 5. N_2 adsorption–desorption isotherms and resulting pore size distribution of γ-Al_2O_3 support and different 12%Ni/γ-Al_2O_3 catalysts.

Table 5
Texture of pure γ-Al_2O_3 support and different 12%Ni/γ-Al_2O_3 catalysts.

Sample	Average pore diameter (nm)	Specific surface area (m^2/g)
Pure γ-Al_2O_3 support	5.8	299.3
Ni/γ-Al_2O_3 (C)	9.8	131.6
Ni/γ-Al_2O_3 (PR)	8.0	153.4
Ni/γ-Al_2O_3 (PC&R)	6.9	173.6

high-temperature process, effectively avoided sintering and plugging, and furthest kept its original feature. Therefore, a higher specific surface area was obtained by plasma process, which benefited the good performance of catalysts.

3.6. TEM analysis

Fig. 6 showed the TEM images of the catalysts. From these images, the smaller size of nickel particle, and the higher nickel dispersion, no obvious sintering and conglomeration were observed for the plasma-activated samples, compared to those

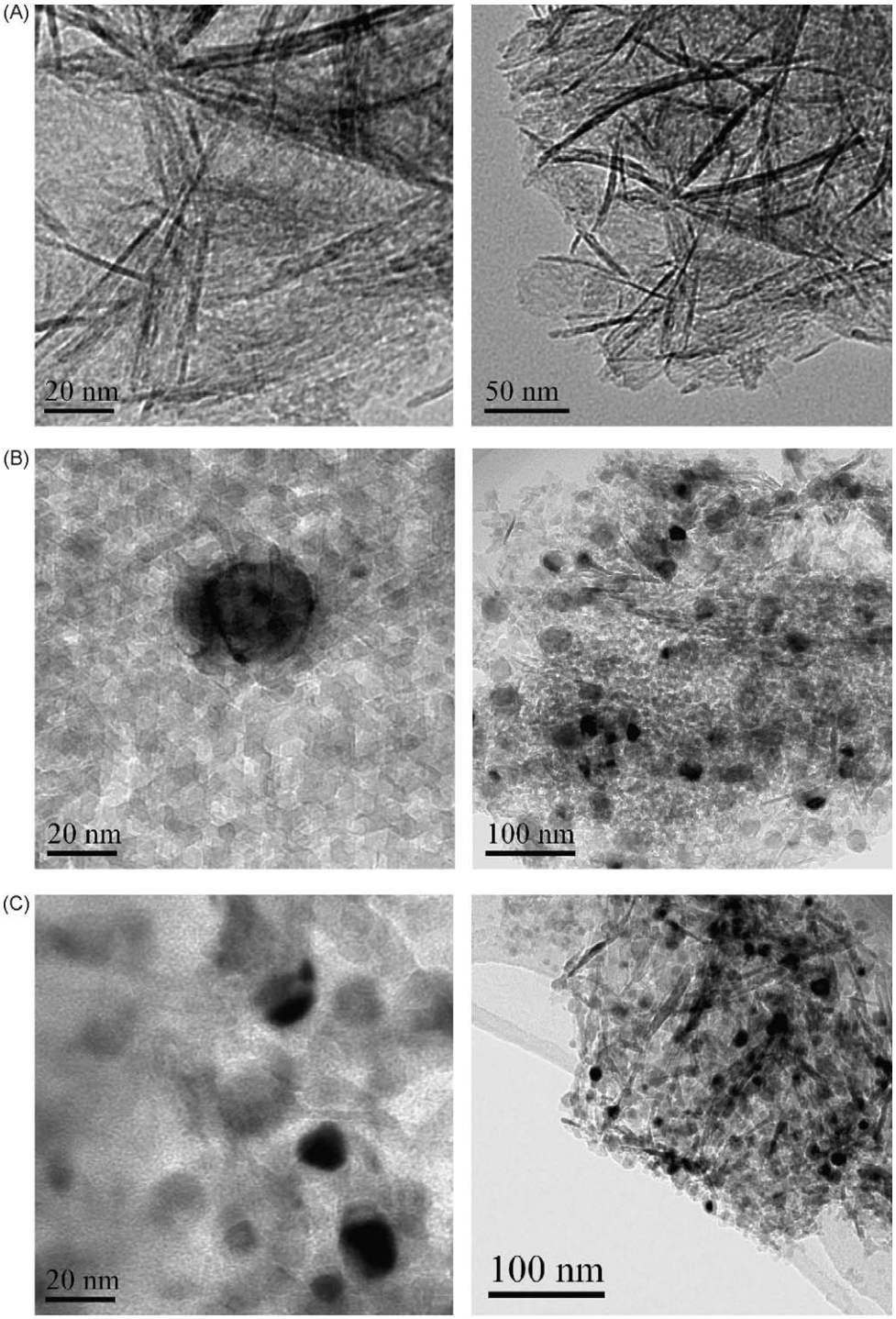

Fig. 6. TEM images of Ni/γ-Al_2O_3. (A) γ-Al_2O_3, (B) Ni/γ-Al_2O_3 (C), (C) Ni/γ-Al_2O_3 (PR) and (D) Ni/γ-Al_2O_3 (PC&R).

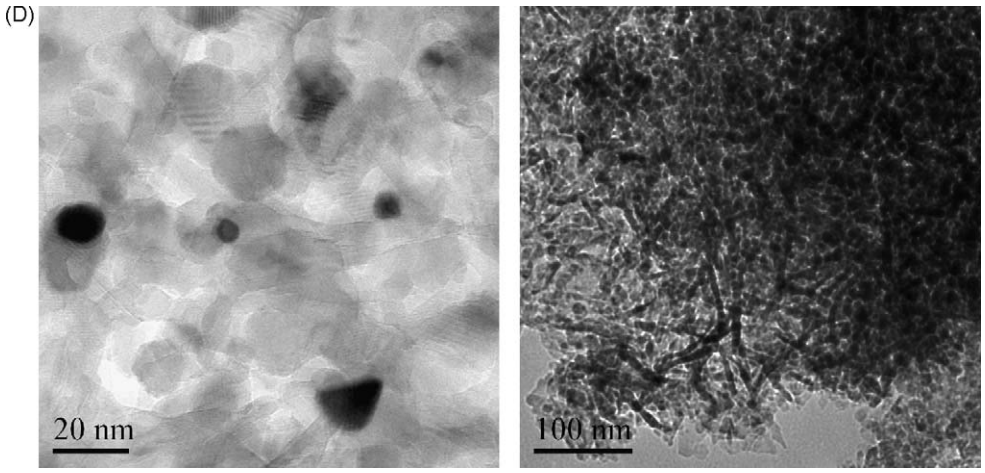

Fig. 6. (*Continued*).

of conventional one. These results well supported the conclusions obtained from the XRD and TPD characterization.

3.7. TGA characterization

Zhang and Verykios [39] reported that three kinds of carbonaceous species formed on the surface of Ni/Al_2O_3 catalyst by TGA, and designated as C_α at 150–220 °C, C_β at 530–600 °C and C_γ at >650 °C. The C_α was an active carbonaceous species which was responsible for the formation of synthesis gas, while C_γ was responsible for catalyst deactivation. The C_β was a surface poison or spectator at low reaction temperature (<530 °C), but they might participate in CO formation, to a small extent, at high temperature (>600 °C). However, the C_β could change into C_γ when time of exposure was longer than 2 h.

The TGA results of $Ni/\gamma\text{-}Al_2O_3$ catalysts after reaction were shown in Fig. 7. The total carbon amount formed on the surface of $Ni/\gamma\text{-}Al_2O_3$ (C) was up to 17.4%, while it was 8.00% for $Ni/\gamma\text{-}Al_2O_3$ (PR) and only 5.84% for $Ni/\gamma\text{-}Al_2O_3$ (PC&R). Especially, most of the carbonaceous species on the surface of $Ni/\gamma\text{-}Al_2O_3$ (PC&R) were the active C_α, and only 0.89% C_β was found. On contrast, on the conventional catalyst, the active C_α and the C_β were 3.87% and 13.53%, respectively. It suggested that the plasma activation induce modifications of the catalyst structure, and the novel catalyst prepared by plasma jet exhibit better anti-carbon deposit performance than that of conventional catalyst. Another surprising

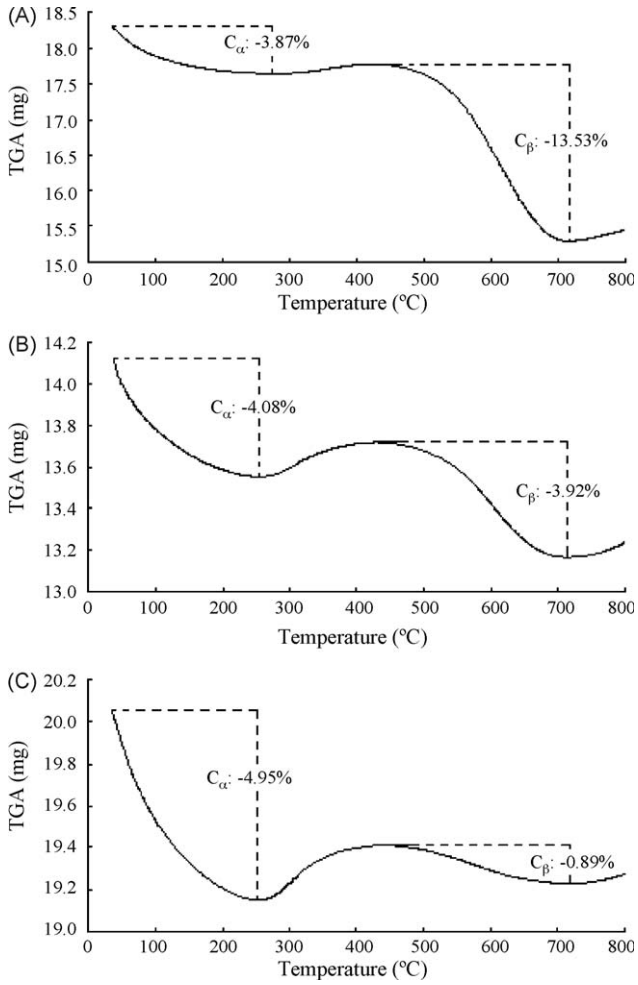

Fig. 7. TGA profile of the conventional and plasma-activated $Ni/\gamma\text{-}Al_2O_3$ catalysts. *Conditions*: Ni loading 12%, reaction temperature = 800 °C, GHSV = 30 L/(g h), CH_4/CO_2 molar ratio = 4/6 and reaction time = 5 h. (A) C, (B) PR and (C) PC&R.

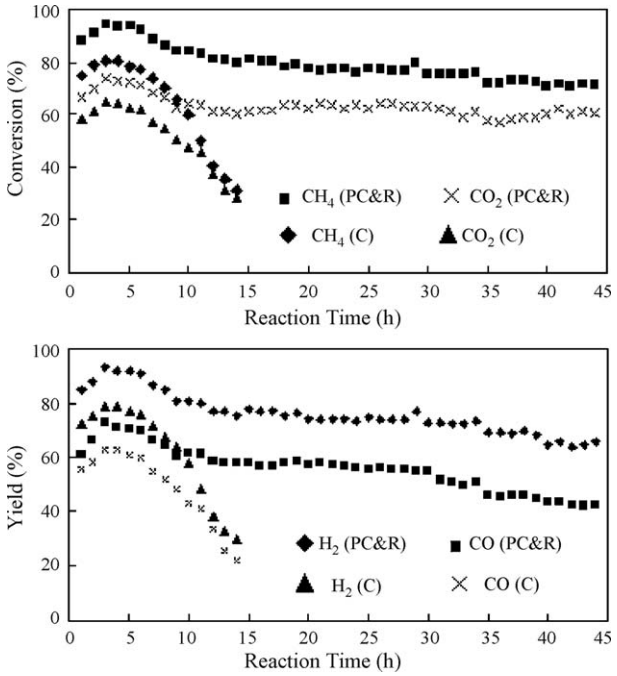

Fig. 8. The stability test results of the conventional and plasma-activated $Ni/\gamma\text{-}Al_2O_3$ (PC&R) catalysts. *Conditions*: catalyst 100 mg, Ni loading 12%, reaction temperature = 800 °C, GHSV = 60 L/(g h) and CH_4/CO_2 molar ratio = 4/6.

thing was that, on the three catalysts, no C_γ can be found. From the results, the sequence of the ability of anti-carbon deposit was: Ni/γ-Al_2O_3 (PC&R) > Ni/γ-Al_2O_3 (PR) > Ni/γ-Al_2O_3 (C). It was agreed with the results obtained by Martinez et al. that Ni particles with diameters below 9 nm would be benefit for resistance of coke formation [5], because the nickel particle size of plasma-assisted Ni/γ-Al_2O_3 (PC&R) sample was only 5 nm in current experiments.

3.8. Stability test results

The stability tests of Ni/γ-Al_2O_3 (C) and Ni/γ-Al_2O_3 (PC&R) were conducted at 800 °C. The results were shown in Fig. 8. Though there is a decrease in activity for both Ni/γ-Al_2O_3 (C) and Ni/γ-Al_2O_3 (PC&R) samples after an initial increase, the conventional Ni/γ-Al_2O_3 catalyst showed a faster deactivation. After 14 h reaction, the CH_4 and CO_2 conversions for Ni/γ-Al_2O_3 (C) changed from 80.3% and 64.4% to 31.5% and 28%, respectively. Similarly, H_2 and CO yields were reduced from 79.1% and 62.9% to 30.0% and 22.1%, respectively. For the Ni/γ-Al_2O_3 (PC&R) catalyst, the decrease rate in conversions and yields was relatively slow after 44 h reaction. It indicated that the Ni/γ-Al_2O_3 (PC&R) catalyst possessed good stability. The stability test results were in agreement with the TGA measurement, as the coke formation was the main reason for catalyst deactivation in CO_2 reforming of CH_4.

4. Conclusions

In this work, a novel plasma-assisted calcination and reduction (PC&R) method was employed to prepare the new Ni/γ-Al_2O_3 catalysts. The catalysts prepared by PC&R method showed a high catalytic activity and an excellent anti-carbon deposit performance in CO_2 reforming of CH_4, it profited from its smaller Ni particle size of only 5 nm, which enhanced nickel dispersion. Both of the smaller Ni particle size and enhanced nickel dispersion profited from the short treatment time of only 10 min in plasma process instead of several hours in conventional calcinations for decomposing and reducing catalyst precursor of Ni$(NO_3)_2$/γ-Al_2O_3. And the short treatment time profited from the action between catalyst precursor and large amount of H atoms in plasma process instead of H_2 in conventional process.

Acknowledgements

This work was supported by the National Natural Science Foundation of China (No. 10475060) and (No. 19935010). The useful discussions of Yuliang Li, Min Xi, Jialiang Liao, Rong Zhao and Li Mei were much appreciated.

References

[1] H.W. Chen, C.Y. Wang, C.H. Yu, L.T. Tseng, P.H. Liao, Catal. Today 97 (2004) 173.
[2] S. Wang, G.Q.M. Lu, J. Chem. Technol. Biotechnol. 75 (2000) 589.
[3] A. Valentini, N.L.V. Carreno, L.F.D. Probst, P.N. Lisboa-Filho, W.H. Schreiner, E.R. Leite, E. Longgo, Appl. Catal. A 255 (2003) 211.
[4] J.S. Choi, K.I. Moon, Y.G. Kim, J.S. Lee, C.H. Kim, D.L. Trimm, Catal. Lett. 52 (1998) 43.
[5] R. Martinez, E. Romero, C. Guimon, R. Bilbao, Appl. Catal. A 274 (2004) 139.
[6] S. Wang, G.Q.M. Lu, Appl. Catal. B 16 (1998) 269.
[7] M.C.J. Bradford, M.A. Vannice, Catal. Rev. Sci. Eng. 41 (1999) 1.
[8] H.Y. Wang, E. Ruckenstein, Appl. Catal. A 204 (2000) 143.
[9] W.D. Zhang, B.S. Liu, Y.L. Tian, Catal. Commun. 8 (2007) 661.
[10] G.H. Liu, W. Chu, H.L. Long, X.Y. Dai, Y.X. Yin, Chin. J. Catal. 28 (2007) 582.
[11] G.H. Liu, Y.L. Li, W. Chu, X.Y. Shi, X.Y. Dai, Y.X. Yin, Catal. Commun. 6 (2008) 1087.
[12] D.G. Cheng, X.L. Zhu, Y.H. Ben, F. He, L. Cui, C.J. Liu, Catal. Today 115 (2006) 205.
[13] G.P. Vissokov, M.I. Panayotova, Catal. Today 72 (2002) 213.
[14] G.P. Vissokov, Catal. Today 98 (2004) 625.
[15] H. Zea, C.K. Chen, K. Lester, A. Phillips, A. Datye, I. Fonseca, J. Phillips, Catal. Today 89 (2004) 237.
[16] H. Shim, J. Phillips, I.M. Fonseca, S. Carabinerio, Appl. Catal. A 237 (2002) 41.
[17] X.L. Zhu, Y.P. Zhang, C.J. Liu, Catal. Lett. 118 (2007) 306.
[18] X.L. Zhu, P.P. Huo, Y.P. Zhang, D.G. Cheng, C.J. Liu, Appl. Catal. B 81 (2008) 132.
[19] Y. Zhao, Y.X. Pan, Y.B. Xie, C.J. Liu, Catal. Commun. 9 (2008) 1558.
[20] Y.X. Pan, C.J. Liu, P. Shi, J. Power Sources 176 (2008) 46.
[21] C.J. Liu, K. Yu, Y.P. Zhang, X.L. Zhu, F. He, B. Eliasson, Catal. Commun. 4 (2003) 303.
[22] Y.P. Zhang, P.S. Ma, X.L. Zhu, C.J. Liu, Y.T. Shen, Catal. Commun. 5 (2004) 35.
[23] Z.J. Wang, Y. Zhao, L. Cui, H. Du, P. Yao, C.J. Liu, Green Chem. 9 (2007) 554.
[24] C.J. Liu, D.G. Cheng, Y.P. Zhang, K.L. Yu, Q. Xia, J.G. Wang, X.L. Zhu, Catal. Surveys Asia 8 (2004) 111.
[25] (a) F. Guo, W. Chu, X.Y. Shi, X. Zhang, Chem. J. Chin. Univ. 30 (2009) 746;
(b) F. Guo, W. Chu, J.Q. Xu, L. Zhong, Chin. J. Chem. Phys. 21 (2008) 481.
[26] Y. Zhang, W. Chu, W.M. Cao, C.R. Luo, X.G. Wen, K.L. Zhou, Plasma Chem. Plasma Process. 20 (2000) 137.
[27] (a) W. Chu, L.N. Wang, P.A. Chernavskii, A.Y. Khodakov, Angew. Chem. Int. Ed. 47 (2008) 5052;
(b) A. Khodakov, W. Chu, P. Fongarland, Chem. Rev. 107 (2007) 1692.
[28] M.H. Chen, W. Chu, X.Y. Dai, X.W. Zhang, Catal. Today 89 (2004) 201.
[29] S.S. Kim, H.W. Lee, B.K. Na, H.K. Song, Catal. Today 89 (2004) 193.
[30] A. Dittmar, H. Kosslick, D. Herein, Catal. Today 89 (2004) 169.
[31] Z.H. Li, S.X. Tian, H.T. Wang, H.B. Tian, J. Mol. Catal. A 211 (2004) 149.
[32] L. Oukacine, F. Gitzhofer, N. Abatzoglou, D. Gravelle, Surf. Coat. Technol. 201 (2006) 2046.
[33] Z.R. Ismagilov, O.Y. Podyacheva, O.P. Solonenko, V.V. Pushkarev, V.I. Kuzmin, V.A. Ushakov, N.A. Rudina, Catal. Today 15 (1999) 411.
[34] F. Pompeo, N.N. Nichio, M.G. Gonzalez, M. Montes, Catal. Today 107–108 (2005) 856.
[35] Q.S. Jing, X.M. Zheng, Energy 31 (2006) 2184.
[36] S. Smeds, T. Salmi, L.P. Lindfors, O. Krause, Appl. Catal. A 144 (1996) 177.
[37] D. Song, J. Li, J. Mol. Catal. A 247 (2006) 206.
[38] C.L. Li, Y.L. Fu, G.Z. Bian, Acta Physico-Chim. Sin. 19 (2003) 902.
[39] Z.L. Zhang, X.E. Verykios, Catal. Today 21 (1994) 589.